Marine Pollution Bulletin 169 (2021) 112582

Contents lists available at ScienceDirect

Marine Pollution Bulletin

journal homepage: www.elsevier.com/locate/marpolbul

Combined effects of climate change and the herbicide diuron on the coral *Acropora millepora*

Florita Flores [a,*], Joseane A. Marques [b], Sven Uthicke [a], Rebecca Fisher [c], Frances Patel [a], Sarit Kaserzon [d], Andrew P. Negri [a]

[a] Australian Institute of Marine Science, Townsville, QLD 4810, Australia
[b] Programa de Pós-Graduação em Oceanografia Biológica, Universidade Federal do Rio Grande, RS, Brazil
[c] Australian Institute of Marine Science, Indian Ocean Marine Research Centre, University of Western Australia, Crawley, WA 6009, Australia
[d] Queensland Alliance for Environmental Health Sciences (QAEHS), The University of Queensland, Woolloongabba, QLD 4102, Australia

ARTICLE INFO

Keywords:
Great Barrier Reef
Climate change
Coral
Herbicide
Ocean acidification
Diuron

ABSTRACT

The Great Barrier Reef (GBR) is threatened by climate change and local pressures, including contaminants in nearshore habitats. This study investigated the combined effects of a GBR-relevant contaminant, the herbicide diuron, under current and two future climate scenarios on the coral *Acropora millepora*. All physiological responses tested (effective quantum yield (ΔF/Fm′), photosynthesis, calcification rate) were negatively affected with increasing concentrations of diuron. Interactive effects between diuron and climate were observed for all responses; however, climate had no significant effect on ΔF/Fm′ or calcification rates. Photosynthesis was negatively affected as the climate scenarios were adjusted from ambient (28.1 °C, pCO_2 = 397 ppm) to RCP8.5 2050 (29.1 °C, pCO_2 = 680 ppm) and 2100 (30.2 °C, pCO_2 = 858 ppm) with EC50 values declining from 19.4 to 10.6 and 2.6 μg L^{-1} diuron in turn. These results highlight the likelihood that water quality guideline values may need to be adjusted as the climate changes.

1. Introduction

Climate change, including ocean warming (OW) and ocean acidification (OA), is a major threat to coral reefs worldwide (Doney et al., 2009; Hoegh-Guldberg et al., 2007; Hughes et al., 2018). Since the pre-industrial era, the global average temperature has increased by about 1 °C (IPCC, 2014; Lough et al., 2018) with a projected increase of 1–3 °C by 2100 (Collins et al., 2013; Knutti et al., 2017). The present-day atmospheric CO_2 (pCO_2) is approximately 400 ppm, with projections of around 900 ppm by the end of the century if no mitigation occurs (Meinshausen et al., 2011; Wuebbles et al., 2017). About a quarter of the CO_2 emitted from anthropogenic sources enters the ocean to produce carbonic acid and causes a myriad of effects (Kroeker et al., 2010), including a reduction in available carbonate ions to marine calcifying organisms (Ganadell et al., 2007; Hoegh-Guldberg et al., 2007).

Many studies have investigated the effects of both OW and OA on marine calcifying organisms, including tropical reef-building corals (Brierley and Kingsford, 2009; Edmunds et al., 2012; Hoegh-Guldberg et al., 2017). One response of corals due to OW is bleaching which is the breakdown in the symbiotic relationship between the coral host and algal symbiont (Goreau and Hayes, 1994), and typically occurs when seawater temperatures are >1 °C above their long-term monthly summer averages for several weeks (Hughes et al., 2017). Bleaching events are becoming more frequent and severe (Hughes et al., 2018) and can negatively affect reproduction (Baird and Marshall, 2002) and cause disease (Bruno et al., 2007) with prolonged and severe bleaching often leading to large-scale coral mortality events (Hughes et al., 2017). OA can also affect corals in several ways, including reduced calcification (Langdon, 2002; Schneider and Erez, 2006) and reduced net productivity (Anthony et al., 2008) as well as having direct and indirect impacts on recruitment (Albright et al., 2008; Anthony et al., 2010).

In addition to the risks posed by climate change, inshore coral reefs may be exposed to a suite of local pressures, including poor water quality caused by coastal development and agricultural activities in adjacent mainland catchments. Along with increased sediment and nutrient loads, pesticides including herbicides, contaminate nearshore ecosystems globally (Bao et al., 2012; Castillo et al., 1997), including the Great Barrier Reef (GBR) (Lewis et al., 2009; O'Brien et al., 2016;

* Corresponding author at: PMB No.3, Townsville MC, Townsville, QLD 4810, Australia.
E-mail addresses: f.flores@aims.gov.au (F. Flores), s.uthicke@aims.gov.au (S. Uthicke), r.fisher@aims.gov.au (R. Fisher), f.patel@aims.gov.au (F. Patel), k.sarit@uq.edu.au (S. Kaserzon), a.negri@aims.gov.au (A.P. Negri).

https://doi.org/10.1016/j.marpolbul.2021.112582
Received 26 January 2021; Received in revised form 12 April 2021; Accepted 26 May 2021

Australian Government and Queensland Government, 2018). During the summer wet season, flood plumes can transport large amounts of agricultural herbicides (>17,000 kg) to the GBR (Kroon et al., 2013); however, due to frequent application and persistence of these herbicides, they have been detected in the GBR catchment area year-round (Gallen et al., 2019; Mercurio et al., 2016). Photosystem II (PSII) herbicides, including diuron (3-(3,4-dichlorophyenyl)-1,1-dimethylurea; DCMU), are the most frequently detected herbicides in the GBR lagoon (Gallen et al., 2019; Lewis et al., 2009; Smith et al., 2012; Warne et al., 2020) and act by blocking the plastoquinone binding site of photosystem II, which disrupts electron transport flow and inhibits photosynthesis, in turn limiting carbon fixation (Oettmeier, 1992). While concentrations of PSII herbicides are highest in freshwater and estuarine ecosystems (Australian Government and Queensland Government, 2018), concentrations of diuron of up to 0.778 μg L^{-1} (average measured concentration over one-month passive sampler deployment) have recently been detected around a nearshore island of the GBR (Gallen et al., 2019), exceeding the proposed PC99 water quality guideline value (WQGV) for diuron (0.43 μg L^{-1}; protection concentration for 99% of species) (Warne et al., 2018) and indicating potential exposure to nearshore coral reef species. Several studies have investigated the effects of diuron on tropical marine phototrophs, including seagrass (Flores et al., 2013; Haynes et al., 2000; Negri et al., 2015), microalgae (Magnusson et al., 2008), coral (Jones and Kerswell, 2003; Jones et al., 2003; Negri et al., 2011) and foraminifera (van Dam et al., 2012). Due to likely exposure and the extensive toxicity dataset that exists for diuron (Warne et al., 2018) this PSII herbicide is commonly used as a reference compound in toxicity bioassays (Thomas et al., 2020a; Thomas et al., 2020b; Wilkinson et al., 2015).

PSII herbicide concentrations in tropical waters are typically highest over the summer wet season (Gallen et al., 2019; Smith et al., 2012); therefore, it is likely that nearshore tropical species, including corals, will be co-exposed to herbicides and high seasonal water temperatures. Studies have already shown that diuron toxicity to corals and their symbionts (Negri et al., 2011), foraminifera (van Dam et al., 2012) and seagrass (Wilkinson et al., 2017) occurs at lower concentrations as temperatures increase. However, this past research has primarily focussed on the effects of PSII herbicides on chlorophyll *a* fluorescence endpoints, such as inhibition of effective quantum yield (ΔF/Fm′), which is proportional to photosynthetic efficiency but may not represent whole-organism responses in symbiotic corals (Ralph et al., 2007). Furthermore, apart from a single study with calcifying tropical marine algae *Halimeda* sp., (Marques et al., 2020), previous investigations on PSII herbicide toxicity to tropical species only tested the influence of OW applicable to current heatwave conditions (Negri et al., 2011) and have not considered the potential influence of combinations of OW and OA relevant to future climate change scenarios. This is the first study to investigate the influence of future climate change conditions (2050 and 2100 RCP8.5 scenario predictions (IPCC, 2014; Meinshausen et al., 2011)) on the toxicity of the GBR-relevant herbicide diuron to a model coral species *Acropora millepora*. The measured responses included photosynthetic efficiency (ΔF/Fm′), net photosynthesis rates, net calcification rates (as a proxy for coral growth) and survival. Holistic experimental approaches such as this can inform regulators on the potential need to adjust water quality guideline values for contaminants as the climate changes (Negri et al., 2020).

2. Methods

2.1. Sample collection

Four adult colonies (30–40 cm diameter) of *Acropora millepora* were collected from Backnumbers Reef (18° 29′ S, 147° 09′ E), GBR under Great Barrier Reef Marine Park Authority (GBRMPA) permit G12/35236.1. Colonies were transported to the National Sea Simulator at the Australian Institute of Marine Science in Townsville and maintained in 1700 L flow-through tanks. Terminal portions of *A. millepora* branches (~2 cm height) were fragmented and affixed on marked glass tiles and maintained in flow-through filtered natural seawater at 27 ± 1 °C under 150–200 μmol m^{-2} s^{-1} (range) for at least one week prior to experimentation. Coral fragments were fed daily with *Artemia* (0.5 nauplii mL^{-1}) during the healing period but were not fed for the duration of the two-week experiment due to possible effects on water quality within the experimental chambers.

2.2. Experimental setup

A. millepora were transferred from acclimation tanks into three climate scenarios (OW + OA): 28.1 ± 0.3 °C and 397 ± 64 ppm pCO_2; 29.1 ± 0.3 °C and 680 ± 90 ppm pCO_2; 30.2 ± 0.3 °C and 858 ± 149 ppm pCO_2 (details are given in Table 1), and five concentrations of diuron (averaged measured: 0.29 ± 0.01, 0.96 ± 0.04, 2.9 ± 0.1, 9.6 ± 0.4 and 29 ± 1 μg L^{-1}, Supporting material Table S1), including a solvent control (measured: below detection limit), in an orthogonal design. Corals (n = 4 replicate coral fragments per chamber) were placed in custom 3 L acrylic chambers (15 cm diameter x 19 cm height, working volume 2.5 L) in temperature-controlled water baths with the appropriate concentration of pCO_2 gently bubbling directly in each chamber. Due to a limited number of experimental chambers, there were no seawater controls (only solvent controls) and there was a 7-day staggered start for corals at 29 μg L^{-1} diuron to maximise number of diuron treatments. pCO_2 dosing was achieved via mass flow controllers (Model GFC17, Aalborg, NY, USA) delivering a precise flow of CO_2 to a series of membrane contactors (Liqui-Cel Extra-Flow 2.5X8, 3M, NC, USA). Analytical grade diuron (>98% purity) was purchased from Sigma-Aldrich (NSW, Australia) and stock solutions (10 mg L^{-1}) were prepared in filtered seawater (0.4 μm) using ethanol as a solvent carrier (<0.03% v/v). Header tanks (60 L) were filled daily with filtered seawater (1 μm) spiked with the appropriate volume of diuron stock to achieve target diuron concentrations. Diuron was delivered from the header tanks to the experimental chambers using peristaltic pumps (Masterflex L/S and Ismatec IPC 12, Cole-Parmer, Vernon Hills, IL, USA) for a turnover rate of 1–1.5 times per day. Three independent replicate chambers were used for each diuron concentration and each climate scenario (a total of 54 chambers). Chambers were randomised within their respective water baths to minimise potential systematic effects of chamber position.

Corals were illuminated over 13 h cycles (LED Hydra, Aqua-Illumination, PA, USA) with ramping up of light intensity for the first 3 h to approximately 200 μmol m^{-2} s^{-1} then down to darkness over the last 3 h (equivalent to 7 mol m^{-2} d^{-1} daily light integral, DLI). Irradiance was measured with a Licor LI-250A meter with LI-190R quantum sensor (Licor, Lincoln, NE, USA). Physico-chemical parameters (pH, salinity and dissolved oxygen) were measured several times over the 15-d experiment (Table 1). Water temperature and pCO_2 levels were controlled by a programmable logic controller (PLC) and measured every 10 min

Table 1
Measured physico-chemical parameters and seawater carbonate chemistry (measured and calculated) during the experimental period. Parameters (mean ± SD) include pH, temperature, salinity and DO. Carbonate chemistry (mean ± SD) includes dissolved inorganic carbon (DIC), total alkalinity (TA), partial pressure of CO_2 (pCO_2) and aragonite saturation state (Ω_{arag}) of each climate condition throughout the duration of the experiment. n denotes sample size.

Parameters	2018	2050	2100
pH (NIST) (n = 96–99)	8.11 ± 0.03	7.94 ± 0.02	7.84 ± 0.05
Temperature (°C) (n = 92–93)	28.1 ± 0.3	29.1 ± 0.3	30.2 ± 0.3
Salinity (n = 32–41)	34.6 ± 0.5	34.6 ± 0.5	34.7 ± 0.4
DO (mg L^{-1}) (n = 36)	7.66 ± 0.1	7.50 ± 0.2	7.40 ± 0.1
DIC (μmol kg^{-1} SW) (n = 6)	2039 ± 14	2136 ± 21	2137 ± 12
TA (μmol kg^{-1} SW) (n = 6)	2291 ± 45	2349 ± 18	2309 ± 18
pCO_2 (ppm) (n = 6)	397 ± 64	680 ± 90	858 ± 149
Ω_{arag} (n = 6)	2.70 ± 0.4	2.61 ± 0.3	2.25 ± 0.1

(Table 1). Salinity was measured via a LAQUAact PC110 meter (Horiba, Kyoto, Japan), pH was measured with a HQ40d equipped with Intellical PHC301 pH electrode (Hach Co., Loveland, CO, USA) and dissolved oxygen concentration was determined with a HQ30d meter equipped with Intellical LDO101 oxygen probe (Hach Co., Loveland, CO, USA).

2.3. Chemical analysis

Analytical samples (2 concentrations plus control per climate scenario) were taken at initiation and termination of experiment. Aliquots (1 mL) were transferred into 1.5 mL liquid chromatography amber glass vials and spiked with a diuron surrogate standard (diuron-d6; stock solution of 1 μg mL^{-1}), of which the final concentration of the surrogate standard was 10 ng mL^{-1}. Diuron concentrations were determined by HPLC-MS/MS (SCIEX Triple Quad 6500 QTRAP mass spectrometer Shimadzu Nexera X2 uHPLC system) at the Queensland Alliance for Environmental Health Sciences (QAEHS), The University of Queensland (Mercurio et al., 2015; Thomas et al., 2020a). The SCIEX software package Analyst Software 1.6 was used for data acquisition and MultiQuant 3.0 was used for quantification. The measured concentrations were calculated based on the linear relationship between nominal and the time weighted average (time = 0 and 15 d) of measured concentrations.

2.4. Seawater carbonate system parameters

Dissolved inorganic carbon (DIC) and total alkalinity (A_T) were determined on a Vindta 3C system (Marianda, Kiel, Germany) from seawater samples taken at the end of the experiment (Table 1). In-house seawater standards and certified reference material (CRM Batch 164 and 174, A.G. Dickson, Scripps Institution of Oceanography, San Diego, CA, USA) were used to validate the accuracy of results. DIC and A_T were used to calculate carbonate system parameters (aragonite saturation state, Ω_{arag}) according to (Mehrbach et al., 1973) with modifications from (Dickson and Millero, 1987) using CO2Sys software (Pierrot et al., 2006).

2.5. Colour index and mortality

Coral fragments were photographed at initiation and 17 days exposure (10 days exposure for 9.6 and 29 μg L^{-1} diuron corals) using a high-resolution digital camera (Nikon D810 with a 60-mm lens and a Nikon Speedlight SB-910 flash). All corals at 29 μg L^{-1} diuron died by 10 days hence could not determine colour index for these individuals. Colour index (proxy for bleaching) was assessed on a random ~0.5 cm^2 square surface area of live coral tissue via the image processing package ImageJ2 (Rueden et al., 2017; Schindelin et al., 2015) as per Bessell-Browne et al. (2017). Briefly, the histogram function in ImageJ2 was used to take the mean grey pixel values (range 0–255) on a black and white scale. Mean grey pixel values were standardised to the minimum and maximum values and converted to a proportion. Complete and partial mortality was also quantified from these images using ImageJ2.

2.6. Chlorophyll fluorescence

Effective quantum yield (ΔF/Fm′) measurements were taken just prior to the start of exposure and after 7 and 14 days of exposure using a pulse amplitude modulation fluorometer (mini PAM, WALZ, Germany; settings: ML = 5, G = 2, D = 2, SI = 8). Two measurements per coral were obtained using a 6-mm fibre optic probe perpendicular to the surface of the coral. Minimum fluorescence was determined by applying a pulse-modulated red measuring light (650 nm, 0.15 μmol photons m^{-2} s^{-1}). A short pulse (800 ms) of saturating actinic light (>3000 μmol photons m^{-2} s^{-1}) was applied to measure light adapted maximum fluorescence. Effective quantum yield was calculated based on *F* and *Fm′* (Genty et al., 1989): $\Delta F/Fm' = (Fm' - F) / Fm'$.

2.7. Net photosynthesis and calcification rates

Corals (n = 3 replicate corals per treatment) used for incubations were chosen at random. Oxygen production and respiration rates, and light and dark calcification rates were determined in corals after 12–15 d exposure for the 0, 0.29, 0.96 and 2.9 μg L^{-1} diuron treatments. Corals exposed to 9.6 μg L^{-1} diuron bleached (and some died) at 10 days exposure, irrespective of the climate scenario. Due to the loss of symbionts and coral tissue rates of oxygen production, respiration and calcification could not be determined for these individuals. Since there was a staggered start for the corals in the 29 μg L^{-1} diuron treatments, these physiological processes were measured after 7–8 d exposure, just prior to bleaching/dying.

To assess net photosynthesis and calcification rates, corals were incubated in the light and dark with respective pCO_2 seawater and diuron treatments in 50 mL clear acrylic chambers for 3 h under experimental light conditions and 4 h dark incubations. Incubation chambers were placed on custom underwater stirrer plates under similar light conditions and water temperature as the experimental chambers. After each incubation, dissolved oxygen concentration (DO) was immediately measured in each incubation chamber, including two blank incubations per treatment as per Strahl et al. (2015). Following dark incubations, corals were snap frozen in liquid nitrogen for future determination of surface area and volume. Surface area of *A. millepora* colonies were determined via wax dipping (Stimson and Kinzie, 1991) and volume of coral was determined using water displacement as per Strahl et al. (2015). Oxygen production and respiration rates (in mg O_2 cm^{-2} h^{-1}) were normalized to surface area:

$$\text{Oxygen production and respiration rates} = \frac{\Delta DO \times (V_{chamber} - V_{coral})}{SA \times T \times 1000}$$

where ΔDO is the difference in DO of blank incubations and incubations with coral (in mg L^{-1}); $V_{chamber}$ is the volume of the incubation chamber (in mL); V_{coral} is the displacement volume of the coral (in mL); SA is the surface area of the coral (in cm^2); and T is the incubation duration (in hours).

Incubation water samples were collected immediately in 50 mL conical centrifuge tubes, fixed with mercuric chloride and analysed for A_T to determine calcification rates by the alkalinity anomaly technique (Chisholm and Gattuso, 1991). A_T was measured on a Metrohm 855 robotic titrosampler (Metrohm, Herisau, Switzerland) by gran titration using 0.5 M HCl using multiple seawater standards and certified reference material (CRM Batch 164 and 174, A.G. Dickson, Scripps Institution of Oceanography, San Diego, CA, USA) as described in Uthicke and Fabricius (2012). Light and dark calcification rates were normalized to surface area:

$$\text{Calcification } \left(\text{in } \mu\text{mol } CaCO_3 \text{ } cm^{-2} \text{ } h^{-1}\right) = \frac{\frac{\Delta TA}{2} \times (V_{chamber} - V_{coral}) \times 1.028}{SA \times T \times 1000}$$

where ΔTA (in μmol kg SW^{-1}); $V_{chamber}$ is the volume of the incubation chamber (in mL); V_{coral} is the displacement volume of the coral (in mL); 1.028 is the density of seawater (in kg L^{-1}); SA is the surface area of the coral (in cm^2); and T is the incubation duration (in hours) (Cohen et al., 2017).

Oxygen production and respiration rates were used to calculate daily net photosynthesis and light and dark calcification rates for daily calcification rates using 13 h of daylight and 11 h of darkness.

2.8. Data analysis

For modelling of relationships, generalized linear mixed models (GLMM) were fitted for each of the coral responses (colour index, ΔF/Fm′, net photosynthesis, daily calcification) with '*Climate*' and '*Diuron*' as the categorical fixed effects and '*Fragment*' as the categorical random factor using the package glmmTMB (Brooks et al., 2017) in R 4.0.3 (R

Core Team, 2020). Colour index and chlorophyll fluorescence data were modelled as a beta distribution using a logit link function (Bessell-Browne et al., 2017) while net photosynthesis and calcification rates were modelled using a gaussian distribution. For all physiological responses, Dunnett's test was used to test for comparisons against the control (2018 climate scenario, 0 μg L^{-1} diuron). Assumptions of normality and homoscedasticity were checked with Shapiro-Wilk test and Levene's test, respectively. Linear regression models were plotted in GraphPad Prism (V7).

Concentrations that decreased colour and inhibited ΔF/Fm′, net photosynthesis and calcification by 50% (EC50) were estimated in R using the package bayesnec (Fisher and Barneche, 2020). This package uses a model averaging approach based on DIC weighted averaged predictions across a potential candidate model set composed of a range of functional NEC models adapted from Fox (2010), along with several more commonly used concentration-response relationship models (Table S2). In all cases model fit was assessed visually through chain mixing, R hat values and an assessment of the number of divergent transitions. Where models showed poor model fit, they were excluded from model averaged estimates of endpoints. EC50 values were calculated using weighted model averaged estimates of all successfully fitted models. Posterior prediction from all successfully fitted models for each response were weighted using pseudo Bayesian Model Averaging method 'pseudobma' via the loo package (Vehtari et al., 2020; Vehtari et al., 2017) with the BB option set to TRUE (i.e. using Bayesian bootstrapping).

ΔF/Fm′ and colour index were modelled as a function of log diuron using Bayesian non-linear models, with the response modelled as a beta distribution. Due to multiple 0 ΔF/Fm′ values for the higher diuron concentrations and since beta distribution are defined on the interval >0 and <1, ΔF/Fm′ was transformed as per Smithson and Verkuilen (2006) whereby if y assumes extremes 0 and 1, a useful transformation is: (y * (n − 1) + 0.5) / n where *n* is the sample size. Both net photosynthesis and daily calcification rates were modelled as a function of log diuron with the response modelled as a gaussian distribution. EC50 values for each climate scenario were directly interpolated from the model averaged posterior predictions using the value halfway between the mean response value for 2018, 0 μg L^{-1} diuron and the mean response value at 2100, 29 μg L^{-1} diuron.

3. Results

Physico-chemical and seawater carbonate chemistry parameters in the treatment chambers over the experimental period are provided in Table 1 and were in the range of the target treatment levels. Measured concentrations of each diuron treatment at each climate scenario were similar (Table S1).

3.1. Colour index and mortality

All corals exposed to 9.6 and 29 μg L^{-1} diuron in the present day and both future climate change scenarios died (complete tissue loss) after 10–11 days exposure. One coral exposed to 2.9 μg L^{-1} diuron in the 2100 climate scenario died and another coral in the same treatment showed 14% partial mortality (data not shown).

Mean grey pixel value of corals at the beginning of the experiment was 93.7 (±13.6 SD). Coral colour was consistent across climate treatments for up to 17 days when exposed to low concentrations of diuron (0 to 0.96 μg L^{-1}) (Fig. 1A, Table S3). However, corals exposed to ≥2.9 μg L^{-1} diuron under 2050 and 2100 were paler in colour than control corals (2018, 0 μg L^{-1}) (Fig. 1A). The corals exposed to 29 μg L^{-1} diuron were not photographed before the mortality event. The modelled concentrations that resulted in 50% colour change (EC50) for each climate (2018, 2050, 2100) were 6.05, 4.99 and 4.86 μg L^{-1}, respectively (Fig. 1A;

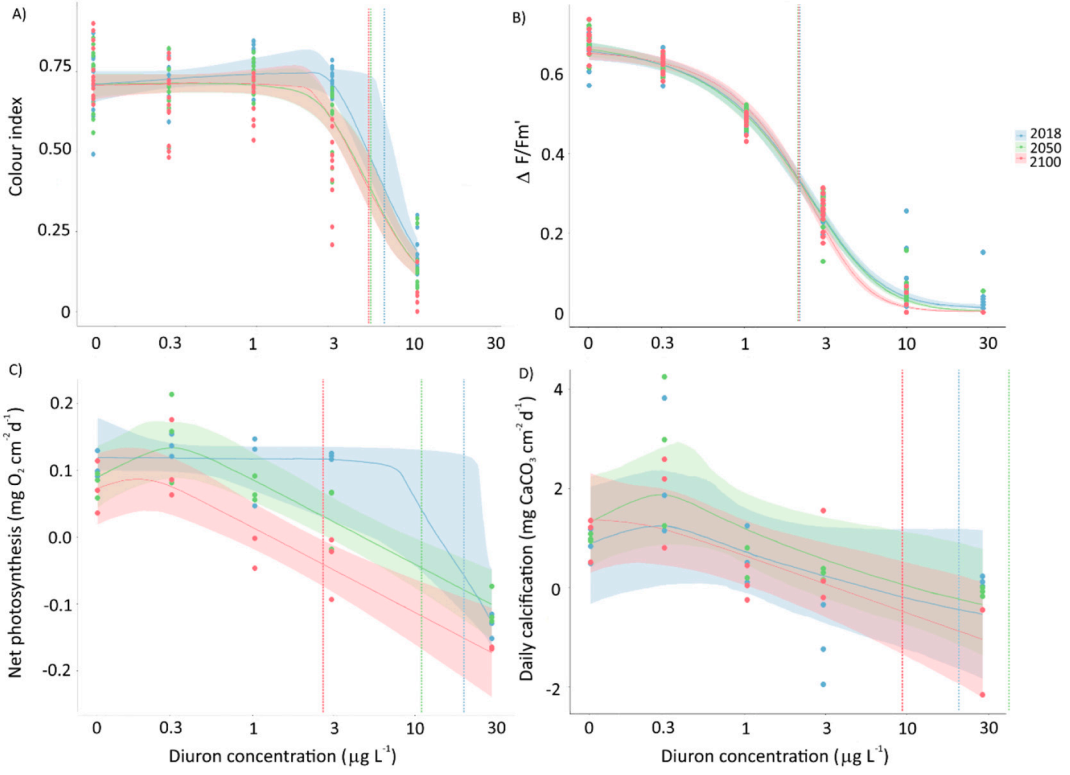

Fig. 1. Concentration-response relationships of A) colour index, B) ΔF/Fm′, C) net photosynthesis and D) daily calcification of *A. millepora* under three climate scenarios and varying concentrations of diuron. Solid lines are Bayesian non-linear beta model fits (colour index and ΔF/Fm′) and gaussian model fits (net photosynthesis and daily calcification) with 95% confidence intervals (shaded areas) used to derive EC50 values (dashed lines). Percent inhibition is relative to control corals (2018, 0 μg L^{-1} diuron).

Table 3). The probability of the colour index EC50 values for the 2050 and 2100 scenarios being less than the 2018 EC50 were 0.956 and 0.970, respectively (Fig. S1.A).

3.2. Effective quantum yield

Control corals (no herbicide) from all climate scenarios exhibited similar ΔF/Fm′ after 7 days (2018: 0.67 ± 0.03 (SD); 2050: 0.67 ± 0.03; 2100: 0.68 ± 0.03; Table S3). These measurements were repeated after 14 d for concentrations up to 2.9 μg L^{-1} and there was no significant difference in ΔF/Fm′ at day 7 and day 14 measurements for each treatment (pairwise *t*-test, $p = 0.678$). ΔF/Fm′ was negatively affected by diuron but not climate scenario (Table 2) and ΔF/Fm′ decreased with increasing diuron concentrations (Fig. 1B). The modelled concentrations that inhibited ΔF/Fm′ by 50% (EC50, in μg L^{-1}) for each climate (2018, 2050, 2100) were 2.06, 2.02 and 2.03, respectively (Fig. 1B; Table 3). Despite a significant interaction term (Table 2), there were no significant differences in these EC50 values, with the probabilities of the 2050 and 2100 EC50 values being different than the 2018 EC50 estimated as 0.615 and 0.539, respectively (Fig. S1.B).

3.3. Net photosynthesis and calcification rates

Net photosynthesis rates were influenced by both climate scenario and diuron, and an interaction was observed (Table 2; Fig. 1C). Photosynthesis was not affected at 0.96 μg L^{-1} diuron under 2018 conditions; however, the same concentration reduced photosynthesis by 35% and 100% under 2050 and 2100 climate conditions, respectively (Fig. 1C). Negative net photosynthesis rates were observed for corals exposed to ≥0.96 μg L^{-1} diuron and under 2100 conditions while this did not occur until 29 μg L^{-1} diuron for corals under 2018 and 2050 conditions (Fig. 1C). Diuron significantly reduced net photosynthesis to levels lower than control (2018, 0 μg L^{-1}) at lower concentrations as the climate scenarios changed: ≥ 29 μg L^{-1} (2018), ≥ 2.9 μg L^{-1} (2050), ≥ 0.29 μg L^{-1} (2100) (Table S3). Oxygen production (from light incubation) was the main contributor to changes in net photosynthesis rates, as dark respiration rates were comparatively consistent across treatments (Fig. S2; Table S3). The approximate diuron concentrations that inhibited net photosynthesis by 50% (EC50, in μg L^{-1}) for each climate (2018, 2050, 2100) were: 19.4, 10.6 and 2.56, respectively (Table 3). The probability of the net photosynthesis EC50 values for the 2050 and 2100 scenarios being less than the 2018 EC50 were 0.861 and 0.997, respectively (Fig. S1.C).

Daily calcification rates were affected by diuron but not by climate scenario and there was a significant interaction between these two factors (Table 2). Daily calcification rates were negatively correlated with diuron concentration; however, substantial increases in calcification rates were observed for corals exposed to 0.29 μg L^{-1} diuron from all climate scenarios (Fig. 1D; Table S3). This corresponded to an average increase of 2.5-fold compared to controls (0 μg L^{-1} diuron). Negative daily calcification rates were observed for corals at ≥2.9 μg L^{-1} diuron (Fig. 1D) though there was high variability in calcification rates of corals under all climate scenarios, potentially explaining the apparent interaction (Fig. 1D; Table S3). Most of the positive calcification across treatments occurred in illuminated corals (Fig. S3, Table S3). The approximate diuron concentrations that inhibited daily calcification by 50% (EC50, in μg L^{-1}) for each climate (2018, 2050, 2100) were 20.6; 42.2 and 9.08, respectively (Table 3). However, the probabilities that daily calcification EC50 values for the 2050 and 2100 scenarios were different to the 2018 EC50 were low: 0.373 and 0.693, respectively (Fig. S1.D).

Table 2
Generalized linear mixed model summary results analysing the effects of climate scenario, diuron and the interaction of the two to chlorophyll fluorescence (ΔF/Fm′), net photosynthesis and daily calcification rates of *A. millepora*. DF: degrees of freedom. Statistically significant (α = 0.05) effects are in bold.

Endpoint	Factor	χ^2	DF	*p*
Colour index	**Climate**	36.2	2	**<0.0001**
	Diuron	638	4	**<0.0001**
	Interaction	58.7	8	**<0.0001**
ΔF/Fm′	Climate	0.291	2	0.29
	Diuron	2786	5	**<0.0001**
	Interaction	51.2	10	**<0.0001**
Net photosynthesis	**Climate**	62.8	2	**<0.0001**
	Diuron	396	4	**<0.0001**
	Interaction	29.4	8	**<0.0001**
Daily calcification	Climate	4.56	2	0.10
	Diuron	105	4	**<0.0001**
	Interaction	21.3	8	**0.0064**

Table 3
Summary of EC50 values (in μg L^{-1}; 95% CI) for colour index, ΔF/Fm′, net photosynthesis and net calcification of *A. millepora* under three climate scenarios and varying concentrations of diuron. NC: not calculable.

	Colour index	ΔF/Fm′	Net photosynthesis	Daily calcification
2018	6.05 (5.28–7.74)	2.06 (1.86–2.24)	19.4 (10.6–29.1)	20.6 (1.76-NC)
2050	4.99 (4.30–6.02)	2.02 (1.88–2.17)	10.6 (5.75–23.7)	42.2 (4.91-NC)
2100	4.86 (4.24–6.0)	2.03 (1.89–2.16)	2.56 (1.39–5.75)	9.08 (2.40-NC)

3.4. Relationships between physiological parameters

ΔF/Fm′ was positively correlated with oxygen production under all climate scenarios (Fig. 2A, Table S4). There were significant linear relationships between light calcification rate and oxygen production rate and between daily calcification and net photosynthesis rates for the 2050 and 2100 climate scenarios (Fig. 2B and C, Table S4).

4. Discussion

The herbicide diuron negatively affected coral survival, coral colour, effective quantum yield (ΔF/Fm′), net photosynthesis and calcification in *Acropora millepora* branches and the effects on coral colour and net photosynthesis were exacerbated by future climate conditions (OW and OA). The effect of diuron was concentration-dependent and no corals survived at ≥9.6 μg L^{-1} diuron for the full two-week exposures in any of the climate scenarios. Net photosynthesis EC50s significantly decreased with increased pCO_2 and temperature; in contrast, ΔF/Fm′ EC50 values were similar under all climate scenarios and while daily calcification EC50 at 2100 was lower than that of 2018 and 2050, there was a high variation in response as shown by the wide confidence intervals of the modelled EC50 values. The increased negative effects of diuron under future climate conditions on net photosynthesis, but not on ΔF/Fm′ or calcification, demonstrates the value of assessing multiple toxicity endpoints and highlights the likelihood that water quality guideline values may need to be adjusted as the climate changes.

4.1. Future climate scenarios tested did not affect coral physiology in the absence of diuron

In the absence of diuron, elevating OW and OA from ambient (28.1 °C, pCO_2 = 397 ppm) to RCP8.5 2050 (29.1 °C, pCO_2 = 680 ppm) and 2100 (30.2 °C, pCO_2 = 858 ppm) conditions had little or no effect on coral colour, ΔF/Fm′, net photosynthesis and calcification in *Acropora millepora* branches. Previous experimental evidence has shown each of these parameters can be affected by OW and OA, but the responses are species-specific and vary considerably with experimental conditions (Ban et al., 2014; Chan and Connolly, 2012; Kornder et al., 2018). Thermal stress from OW alone can cause oxidative damage to PSII in

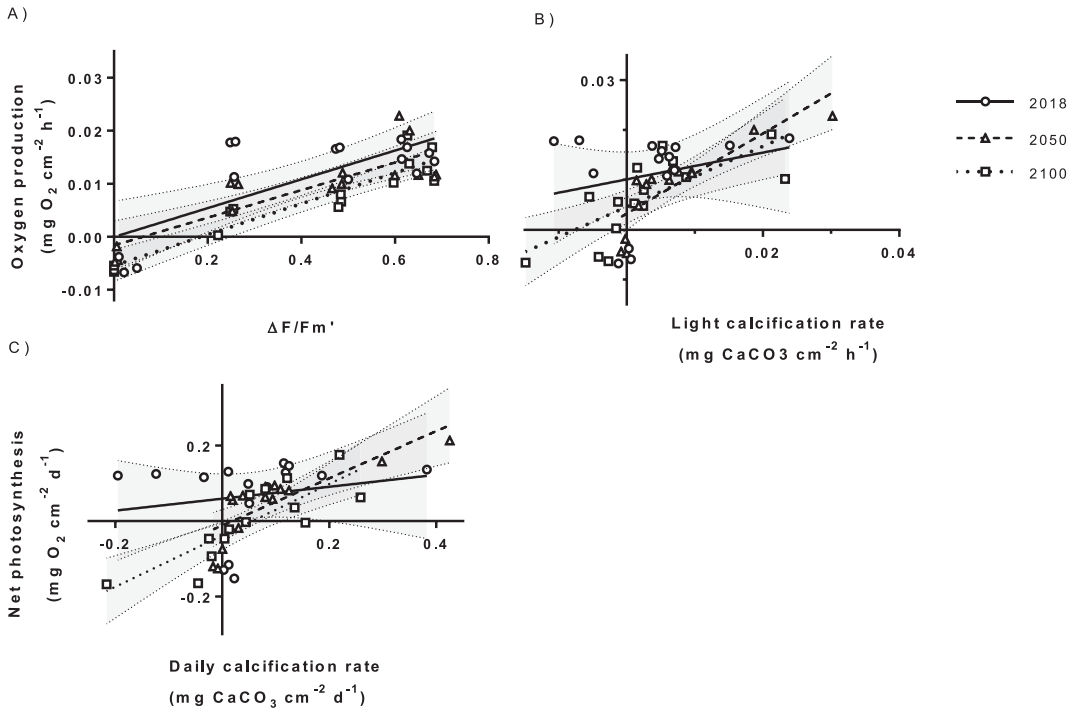

Fig. 2. Regression models (±95% CI) of A) effective quantum yield (ΔF/Fm′) and oxygen production, B) light calcification rate and oxygen production and C) daily calcification rate and net photosynthesis for *A. millepora* under three climate scenarios and elevated diuron concentrations. Slopes and goodness of fit values are in Table S4.

symbionts which leads to reduced ΔF/Fm′, limiting electron transport and reducing oxygen production, and when combined with thermal effects on respiration, reduces net photosynthesis (Coles and Jokiel, 1977; Lesser, 2011). Calcification rates were higher in the light than in the dark due to light-enhanced calcification (Goreau, 1959; Kawaguti and Sakumoto, 1948), but thermal stress can suppress light-enhanced calcification due to effects on photosynthesis (stress on PSII and loss of symbionts) (Langdon and Atkinson, 2005). OA, on the other hand, can affect calcification due to reduced dissolved inorganic carbon (Langdon and Atkinson, 2005), but its direct effects on PSII and ΔF/Fm′ and net photosynthesis are less clear and can be either enhanced or suppressed (Noonan and Fabricius, 2016). The effects of OA and OW have generally been shown to be exacerbated by experimental combinations of these pressures (Anthony et al., 2008), but the previously applied conditions have usually been more severe than those applied in the present study, likely explaining the lack of effect observed on ΔF/Fm′, net photosynthesis and calcification in *A. millepora* branches (in the absence of diuron) here. Furthermore, the exposure duration was relatively brief in the current study, and corals may have had adequate energy resources to continue to calcify in the short-term under increased pCO_2 conditions.

4.2. Effects of diuron alone on A. millepora

Diuron had clear concentration-dependent effects on ΔF/Fm′, exhibiting EC50s (2.02–2.06 μg L^{-1}), similar to those reported in other coral studies (2.3–6 μg L^{-1}) (Jones and Kerswell, 2003; Jones et al., 2003; Negri et al., 2011), reinforcing the sensitivity of this photophysiological endpoint. Diuron also affected coral colour, net photosynthesis and calcification rates with higher EC50s predicted; however, the EC50s for calcification had wide confidence intervals and should be considered preliminary. Similar concentrations or chronic exposures can lead to coral bleaching (Cantin et al., 2007; Jones et al., 2003; Negri et al., 2005), decreased lipid content, reproductive output and mortality (Cantin et al., 2007). While the effect of diuron on ΔF/Fm′ in corals is almost immediate and does not change over prolonged periods, bleaching and whole organism effects, such as suppression of growth, are likely to become more severe over sustained exposures (Cantin et al., 2007). Reduced calcification in corals due to herbicide exposure has been reported previously in *Pocillopora damicornis* colonies (Vandermeulen et al., 1972), with suppression of light-enhanced calcification the likely mechanism. As a proxy for growth, inhibition of calcification should be investigated further as an ecologically relevant endpoint for the effects of contaminants on corals. The EC50s in this study (2.02–42.2 μg L^{-1}) were higher than diuron concentrations commonly detected in the GBR, for example, the highest concentration detected in a recent monitoring was 0.778 μg L^{-1} diuron (Gallen et al., 2019). While EC10 values would be lower and more appropriate for comparison against environmental values and water quality guidelines, they were not presented here due to very wide confidence intervals.

4.3. The influence of future climate scenarios on diuron toxicity

This is the first study to investigate the effects of both the global pressure of climate change (OW and OA) and the local pressure of the herbicide diuron on corals. ΔF/Fm′ was negatively affected by diuron across all climate scenarios and inhibition of ΔF/Fm′ was nearly identical at low diuron concentrations among scenarios. While interactive effects of climate and diuron were observed for ΔF/Fm′, this significant interaction was most likely due to the near complete suppression in ΔF/Fm′ at the two highest diuron concentrations, thus similar EC50 values were estimated for all three climate scenarios.

Diuron acts by blocking electron transport in Photosystem II which under illumination causes an increase in chlorophyll fluorescence and a reduction in ΔF/Fm′ (Genty et al., 1989), and this correlated with reduced oxygen production in the current study (Fig. 2A). The ΔF/Fm′ EC50 was lower than that of net photosynthesis under 2018 climate conditions. However, net photosynthesis was far more suppressed by diuron under the 2100 scenario and the similar EC50s for ΔF/Fm′ and net photosynthesis indicated close to a 1:1 link between the reduction of electron transport and net photosynthesis by diuron under these

conditions. There were strong negative and interactive effects of both future climate scenarios and diuron on net photosynthesis. This influence of OW and OA on suppressing net photosynthesis in the presence of diuron was primarily due to the net effects on oxygen production and/or respiration under illuminated conditions (Fig. S2) indicating light also plays a role, but it is uncertain whether the influence affects oxygen production, respiration or both.

Symbiont density was not determined; instead, bleaching was assessed through colour changes via colour indexing techniques (Bessell-Browne et al., 2017; Siebeck et al., 2006). The paling of corals over time was most likely caused by a loss of symbionts and gradual depletion of chlorophyll (Anthony et al., 2008). OW and OA heightened bleaching effects in the presence of diuron by disrupting the photoprotective mechanisms of coral symbionts (Anthony et al., 2008) and under herbicidal stress, the inhibition of photochemical efficiency probably led to a dissociation of symbionts and visible bleaching of the coral (Jones and Kerswell, 2003).

Diuron concentrations $\geq$2.9 μg L^{-1} reduced daily calcification to below zero (=net dissolution) in all climate scenarios. This is likely to be driven by suppression of light-enhanced calcification as calcification was only affected in illuminated corals (Fig. S3) and the effects on light calcification rate and oxygen production were well correlated (Fig. 2B). The diuron EC50s for net calcification were generally higher than for ΔF/Fm′ and net photosynthesis indicating that despite the herbicide reducing photosynthesis, the corals likely maintained an intracellular pool of available dissolved inorganic carbon required for calcification (Langdon and Atkinson, 2005) over the short exposure period. While the 2100 EC50 was lower than that of the 2018 scenario, indicating possible exacerbation of future climate scenarios on calcification, the data were too inconsistent and confidence intervals were too wide to support this conclusion. Additionally, there was a limitation of sample size in this study and an increase in sample size may have better defined the trend and/or influence of climate on calcification. The thermal stress applied in the future climate scenarios (up to +2 °C for less than two weeks) was below the bleaching threshold for *A. millepora* in all the diuron/climate treatments. However, thermal bleaching of *A. millepora* at higher temperatures (+5 °C) is enhanced by diuron exposure (Negri et al., 2011) and reduced calcification rates have been observed in bleached corals (Goreau, 1959; Goreau and Goreau, 1959; Kawaguti and Sakumoto, 1948). These types of interactions are more likely to be evident over prolonged co-exposures to PSII herbicides during heatwaves or under future climate conditions.

4.4. Enhanced calcification at low diuron concentrations

Enhanced calcification and to a lesser extent net photosynthesis, were observed for corals exposed to 0.29 μg L^{-1} diuron across all climate scenarios. The phenomenon that low concentrations of a chemical can induce a beneficial effect while damaging effects are observed at higher concentrations (a stimulatory hormetic-like response) has been intensively studied (Calabrese and Blain, 2005; Duke et al., 2006). A review of 5600 concentration-response relationships by Calabrese and Blain (2005) found that the maximum stimulatory response (e.g. growth, longevity, metabolic parameters) was usually less than two-fold greater than the control. In this study, calcification rates in corals at 0.29 μg L^{-1} diuron were an average of 2.5-fold higher than the rates of control corals which is well within the range found in the review (>10-fold stimulation in growth was not uncommon). Additionally, Roubeix et al. (2011) found low to moderate concentrations of diuron (<5 μg L^{-1}) stimulated growth of several species of periphytic diatoms through acute laboratory ecotoxicological assays. Other PSII herbicides have been found to have stimulatory effects, including simazine (10–160 μg L^{-1}) which increased protein content in rye plants (Ries et al., 1967) and increased protein content in the roots of barley (Pulver and Ries, 1973). These stimulatory responses in calcification and photosynthesis may be linked since light-enhanced calcification is largely photosynthesis dependent (Vandermeulen et al., 1972). Diuron is a phenylurea herbicide, and previous studies have shown that carbon (^{14}C) in urea is incorporated into skeletal carbonate of corals (Crossland and Barnes, 1974). Biscéré et al. (2018) observed enhanced photosynthetic and calcification rates in coral with urea enrichment. Urease, which is found in both coral host and algal symbionts (Barnes and Crossland, 1976) catalyses the hydrolysis of urea to produce inorganic carbon and ammonia (Krajewska, 2009). Ammonia then neutralizes the protons formed during calcification and shifts the equilibrium towards the precipitation of $CaCO_3$, enhancing calcification (Biscéré et al., 2018). It is possible that stimulation of calcification by low concentrations of diuron could occur if this herbicide acts as a source of urea. However, the biochemical transformation of diuron into free urea has not yet been described (Moretto et al., 2019) and further research is needed to understand the mechanism underlying the observation that low concentrations of diuron can enhance calcification by an average of more than two-fold across all climate treatments.

5. Conclusion

The increased effects of diuron under future climate conditions on net photosynthesis but not on ΔF/Fm′ or calcification demonstrates the value of assessing multiple toxicity endpoints. Many previous studies on the effects of herbicides such as diuron on corals have relied on ΔF/Fm′ inhibition as a toxicity endpoint (Jones and Kerswell, 2003; Jones et al., 2003; Negri et al., 2011); however, additional stressors such as OA and OW can also influence other important physiological functions. Measuring whole-organism responses, such as net photosynthesis, is needed to reveal the potential enhanced toxicity of diuron under future climate scenarios. While climate-enhanced effects of diuron on calcification were not significant, the links between oxygen production and light calcification indicates that over prolonged exposures skeletal growth in corals may be more vulnerable to climate change in the presence of contaminants that suppress photosynthesis, like diuron. This study supports the management of contaminants to improve coral reef resilience to climate change (Australian Government and Queensland Government, 2018) and adjustments to water quality guideline values to account for future climate conditions may need to be considered to ensure future protection of marine ecosystems (Negri et al., 2020).

CRediT authorship contribution statement

Florita Flores: Conceptualization, Investigation, Data curation, Formal analysis, Writing – original draft. **Joseane A. Marques:** Conceptualization, Investigation, Data curation, Formal analysis, Writing – review & editing. **Sven Uthicke:** Conceptualization, Formal analysis, Writing – review & editing. **Rebecca Fisher:** Formal analysis, Writing – review & editing. **Frances Patel:** Investigation, Writing – review & editing. **Sarit Kaserzon:** Formal analysis, Writing – review & editing. **Andrew P. Negri:** Conceptualization, Formal analysis, Writing – review & editing.

Declaration of competing interest

The authors declare that they have no known competing financial interests or personal relationships that could have appeared to influence the work reported in this paper.

Acknowledgements

The authors thank the staff at the National Sea Simulator at AIMS for assistance with experimental setup and field assistance. Additional thanks to Paul Kurtenbach and Marie Thomas for assistance with sample processing. The authors acknowledge the Manbarra and Bindal People as the Traditional Owners where this work took place. We pay our respects to their Elders past, present and emerging and we acknowledge

their continuing spiritual connection to their land and sea country. This research was supported by the Australian Government's National Environmental Science Program (NESP) Tropical Water Quality Hub Project 2.1.6 and 5.2.

References

Albright, R., Mason, B., Langdon, C., 2008. Effect of aragonite saturation state on settlement and post-settlement growth of *Porites astreoides* larvae. Coral Reefs 27, 485–490.

Anthony, K.R.N., Kline, D.I., Diaz-Pulido, G., Dove, S., Hoegh-Guldberg, O., 2008. Ocean acidification causes bleaching and productivity loss in coral reef builders. Proc. Natl. Acad. Sci. 105, 17442–17446.

Anthony, K.R.N., Maynard, J.A., Diaz-Pulido, G., Mumby, P.J., Marshall, P., Cao, L., Hoegh-Guldberg, O., 2010. Ocean acidification and warming will lower coral reef resilience. Glob. Chang. Biol. 17, 1798–1808.

Australian Government and Queensland Government, 2018. Reef 2050 Water Quality Improvement Plan 2017–2022. Australian and Queensland Government. https://www.reefplan.qld.gov.au/_data/assets/pdf_file/0017/46115/reef-2050-water-quality-improvement-plan-2017-22.pdf.

Baird, A.H., Marshall, P.A., 2002. Mortality, growth and reproduction in scleractinian corals following bleaching on the Great Barrier Reef. Mar. Ecol. Prog. Ser. 237, 133–141.

Ban, S.S., Graham, N.A., Connolly, S.R., 2014. Evidence for multiple stressor interactions and effects on coral reefs. Glob. Chang. Biol. 20, 681–697.

Bao, L.J., Maruya, K.A., Snyder, S.A., Zeng, E.Y., 2012. China's water pollution by persistent organic pollutants. Environ. Pollut. 163, 100–108.

Barnes, D.J., Crossland, C.J., 1976. Urease activity in the staghorn coral, *Acropora acuminata*. Comp. Biochem. Physiol. 55B, 371–376.

Bessell-Browne, P., Negri, A.P., Fisher, R., Clode, P.L., Duckworth, A., Jones, R., 2017. Impacts of turbidity on corals: the relative importance of light limitation and suspended sediments. Mar. Pollut. Bull. 117, 161–170.

Biscéré, T., Ferrier-Pagès, C., Grover, R., Gilbert, A., Rottier, C., Wright, A., Payri, C., Houlbrèque, F., 2018. Enhancement of coral calcification via the interplay of nickel and urease. Aquat. Toxicol. 200, 247–256.

Brierley, A.S., Kingsford, M.J., 2009. Impacts of climate change on marine organsims and ecosystems. Curr. Biol. 19, R602–R614.

Brooks, M.E., Kristensen, K., van Benthem, K.J., Magnusson, A., Berg, C.W., Nielsen, A., Skaug, H.J., Mächler, M., Bolker, B.M., 2017. glmmTMB balances speed and flexibility among packages for zero-inflated generalized linear mixed modeling. The R Journal 9 (2), 378–400.

Bruno, J.F., Selig, E.R., Casey, K.S., Page, C.A., Willis, B.L., Harvell, C.D., Sweatman, H., Melendy, A.M., 2007. Thermal stress and coral cover as drivers of coral disease outbreaks. PLoS Biol. 5, e124.

Calabrese, E.J., Blain, R., 2005. The occurrence of hormetic dose responses in the toxicological literature, the hormesis database: an overview. Toxicol. Appl. Pharmacol. 202, 289–301.

Cantin, N.E., Negri, A.P., Willis, B.L., 2007. Photoinhibition from chronic herbicide exposure reduces reproductive output of reef-building corals. Mar. Ecol. Prog. Ser. 344, 81–93.

Castillo, L.E., de la Cruz, E., Ruepert, C., 1997. Ecotoxicology and pesticides in tropical aquatic ecosystems of Central America. Environ. Toxicol. Chem. 16, 41–51.

Chan, N.C.S., Connolly, S.R., 2012. Sensitivity of coral calcification to ocean acidification: a meta-analysis. Glob. Chang. Biol. 19, 282–290.

Chisholm, John R.M., Gattuso, Jean-Pierre, 1991. Validation of the alkalinity anomaly technique for investigating calcification of photosynthesis in coral reef communities. Limnol. Oceanogr. 36 https://doi.org/10.4319/lo.1991.36.6.1232.

Cohen, S., Krueger, T., Fine, M., 2017. Measuring coral calcification under ocean acidification: methodological considerations for the ^{45}Ca-uptake and total alkalinity anomaly technique. PeerJ 5, e3749.

Coles, S.L., Jokiel, P.L., 1977. Effects of temperature on photosynthesis and respiration in hermatypic corals. Mar. Biol. 43, 209–216.

Collins, M., Knutti, R., Arblaster, J., Dufresne, J.-L., Fichefet, T., Friedlingstein, P., Gao, X., Gutowski, W.J., Johns, T., Krinner, G., Shongwe, M., Tebaldi, C., Weaver, A.J., Wehner, M., 2013. Long-term climate change: projections, commitments and irreversibility, in: Stocker, T.F., Qin, D., Plattner, G.-K., Tignor, M., Allen, S.K., Doschung, J., Nauels, A., Xia, Y., Bex, V., Midgley, P.M. (Eds.), Climate Change 2013: The Physical Science Basis. Contribution of Working Group I to the Fifth Assessment Report of the Intergovernmental Panel on Climate Change. Cambridge University Press, Cambridge, UK, pp. 1029–1136.

Crossland, C.J., Barnes, D.J., 1974. The role of metabolic nitrogen in coral calcification. Mar. Biol. 28, 325–332.

Dickson, A.G., Millero, F.J., 1987. A comparison of the equilibrium constants for the dissociation of carbonic acid in seawater media. Deep Sea Res. Part A 34, 1733–1743.

Doney, S.C., Fabry, V.J., Feely, R.A., Kleypas, J.A., 2009. Ocean acidification: the other CO_2 problem. Annu. Rev. Mar. Sci. 1, 169–192.

Duke, S.O., Cedergreen, N., Velini, E.D., Gelz, R.G., 2006. Hormesis: is it an important factor in herbicide use and allelopathy? Outlooks Pest Manag. 17, 29–33.

Edmunds, P.J., Brown, D., Moriarty, V., 2012. Interactive effects of ocean acidification and temperature on two scleractinian corals from Moorea, French Polynesia. Glob. Chang. Biol. 18, 2173–2183.

Fisher, R., Barneche, D.R., 2020. The R-package bayesnec, https://github.com/open-AIMS/bayesnec, accessed 17/11/2020, commit: 965f5b4e8d2f5964b18c9c37523711b07585d43a.

Flores, F., Collier, C.J., Mercurio, P., Negri, A., 2013. Phytotoxicity of four photosystem II herbicides to tropical seagrasses. PLoS One 8, e75798.

Fox, D.R., 2010. A Bayesian approach for determining the no effect concentration and hazardous concentration in ecotoxicology. Ecotoxicol. Environ. Saf. 73, 123–131.

Gallen, C., Thai, P., Paxman, C., Prasad, P., Elisei, G., Reeks, T., Eaglesham, G., Yeh, R., Tracey, D., Grant, S., Mueller, J.F., 2019. Marine Monitoring Program: Annual Report for Inshore Pesticide Monitoring 2017–18, Report for the Great Barrier Reef Marine Park Authority, Great Barrier Reef Marine Park Authority, Townsville, 118 pp.

Ganadell, J.G., Le Quéré, C., Raupach, M.R., Field, C.B., Buitenhuis, E.T., Ciais, P., Conway, T.J., Gillett, N.P., Houghton, R.A., Marland, G., 2007. Contributions to accelerating atmospheric CO_2 growth from economic activity, carbon intensity, and efficiency of natural sinks. Proc. Natl. Acad. Sci. 104, 18866–18870.

Genty, B., Briantais, J.M., Baker, N.R., 1989. The relationship between the quantum yield of photosynthetic electron transport and quenching of chlorophyll fluorescence. Biochim. Biophys. Acta Gen. Subj. 990, 87–92.

Goreau, T.F., 1959. The physiology of skeleton formation in corals. I. A method for measuring the rate of calcium deposition by corals under different conditions. Biol. Bull. 116, 59–75.

Goreau, T.F., Goreau, N.I., 1959. The physiology of skeleton formation in corals. II. Caclcium deposition by hermatypic corals under various conditions in the reef. Biol. Bull. 117, 239–250.

Goreau, T.J., Hayes, R.L., 1994. Coral bleaching and ocean "hot spots". Ambio 23, 176–180.

Haynes, D., Ralph, P., Prange, J., Dennison, B., 2000. The impact of the herbicide diuron on photosynthesis in three species of tropical seagrass. Mar. Pollut. Bull. 41, 288–293.

Hoegh-Guldberg, O., Mumby, P.J., Hooten, A.J., Steneck, R.S., Greenfield, P., Gomez, E., Harvell, C.D., Sale, P.F., Edwards, A.J., Caldeira, K., Knowlton, N., Eakin, C.M., Iglesias-Prieto, R., Muthiga, N., Bradbury, R.H., Dubi, A., Hatziolos, M.E., 2007. Coral reefs under rapid climate change and ocean acidification. Science 318, 1737–1742.

Hoegh-Guldberg, O., Poloczanska, E.S., Skirving, W., Dove, S., 2017. Coral reef ecosystems under climate change and ocean acidification. Front. Mar. Sci. 4, 158.

Hughes, T.P., Kerry, J.T., Álvarez-Noriega, M., Álvarez-Romero, J.G., Anderson, K.D., Baird, A.H., Babcock, R.C., Beger, M., Bellwood, D.R., Berkelmans, R., Bridge, T.C., Butler, I.R., Byrne, M., Cantin, N.E., Comeau, S., Connolly, S.R., Cumming, G.S., Dalton, S.J., Diaz-Pulido, G., Eakin, C.M., Figueira, W.F., Gilmour, J.P., Harrison, H. B., Heron, S.F., Hoey, A.S., Hobbs, J.A., Hoogenboom, M.O., Kennedy, E.V., Kuo, C. Y., Lough, J.M., Lowe, R.J., Liu, G., McCulloch, M.T., Malcolm, H.A., McWilliam, M. J., Pandolfi, J.M., Pears, R.J., Pratchett, M.S., Schoepf, V., Simpson, T., Skirving, W. J., Sommer, B., Torda, G., Wachenfeld, D.R., Willis, B.L., Wilson, S.K., 2017. Global warming and recurrent mass bleaching of corals. Nature 543, 373–377.

Hughes, T.P., Anderson, K.D., Connolly, S.R., Heron, S.F., Kerry, J.T., Lough, J.M., Baird, A.H., Baum, J.K., Berumen, M.L., Bridge, T.C., Claar, D.C., Eakin, C.M., Gilmour, J.P., Graham, N.A.J., Harrison, H., Hobbs, J.-P.A., Hoey, A.S., Hoogenboom, M., Lowe, R.J., McCulloch, M.T., Pandolfi, J.M., Pratchett, M., Schoepf, V., Torda, G., Wilson, S.K., 2018. Spatial and temporal patterns of mass bleaching of corals in the Anthropocene. Science 359, 80–83.

IPCC, 2014. Climate Change 2014: Synthesis Report. Contribution of Working Groups I, II and II to the Fifth Assessment Report of Intergovernmental Panel on Climate Change [Core writing team, R.K. Pachauri and L.A. Meyer (eds)]. IPCC, Geneva, Switzerland, 151 pp.

Jones, R.J., Kerswell, A.P., 2003. Phytotoxicity of photosystem II (PSII) herbicides to coral. Mar. Ecol. Prog. Ser. 261, 149–159.

Jones, R.J., Muller, J., Haynes, D., Schreiber, U., 2003. Effects of herbicides diuron and atrazine on corals of the Great Barrier Reef, Australia. Mar. Ecol. Prog. Ser. 251, 153–167.

Kawaguti, S., Sakumoto, D., 1948. The effect of light on the calcium deposition of corals. Bull. Oceanogr. Inst. Taiwan 4, 65–70.

Knutti, R., Rugenstein, M.A.A., Hegerl, G.C., 2017. Beyond equilibrium climate sensitivity. Nat. Geosci. 10, 727–736.

Kornder, N.A., Riegl, B.M., Figueiredo, J., 2018. Thresholds and drivers of coral calcification responses to climate change. Glob. Chang. Biol. 24, 5084–5095.

Krajewska, B., 2009. Ureases I. functional, catalytic and kinetic properties: a review. J. Mol. Catal. B Enzym. 59, 9–21.

Kroeker, K.J., Kordas, R.L., Crim, R.N., Singh, G.G., 2010. Meta-analysis reveals negative yet variable effects of ocean acidification on marine organisms. Ecol. Lett. 13, 1419–1434.

Kroon, F., Turner, R., Smith, R., Warne, M.St.J., Hunter, H., Bartley, R., Wilkinson, S., Lewis, S., Waters, D., Carroll, C., 2013. Scientific Consensus Statement. Chapter 4 - sources of sediment, nutrients, pesticides and other pollutants in the Great Barrier Reef catchment. Reef Water Quality Protection Plan Secretariat, Brisbane, Queensland. 42p. Available from: http://www.reefplan.qld.gov.au/about/scientific-consensus-statement/sources-of-pollutants.aspx.

Langdon, C., 2002. Review of experimental evidence for effects of CO2 on calcification of reef builders, Proc 9th Int Coral Reef Symp, pp. 1091–1198.

Langdon, C., Atkinson, M.J., 2005. Effect of elevated pCO_2 on photoysnthesis and calcification of corals and interaction with seasonal change in temperature/irradiance and nutrient enrichment. J. Geophys. Res. C Oceans 110, 1–16.

Lesser, M.P., 2011. Coral bleaching: causes and mechanisms, in: Dubinsky, Z., Stambler, N. (Eds.), Coral Reefs: An Ecosystem in Transition. Springer Netherlands, pp. 405–419.

Lewis, S.E., Brodie, J.E., Bainbridge, Z.T., Rohde, K.W., Davis, A.M., Masters, B.L., Maughan, M., Devlin, M.J., Mueller, J.F., Schaffelke, B., 2009. Herbicides: a new threat to the Great Barrier Reef. Environ. Pollut. 157, 2470–2484.
Lough, J., Anderson, K., Hughes, T., 2018. Increasing thermal stress for tropical coral reefs: 1871–2017. Sci. Rep. 8, 6079.
Magnusson, M., Heimann, K., Negri, A.P., 2008. Comparative effects of herbicides on photosynthesis and growth of tropical estuarine microalgae. Mar. Pollut. Bull. 56, 1545–1552.
Marques, J.A., Flores, F., Patel, F., Bianchini, A., Uthicke, S., Negri, A.P., 2020. Acclimation history modulates effect size of calcareous algae (*Halimeda opuntia*) to herbicide exposure under future climate scenarios. Sci. Total Environ. 739, 140308.
Mehrbach, C., Culberson, C.H., Hawley, J.E., Pytkowicz, R.M., 1973. Constants of carbonic acid in seawater at atmospheric pressure. Limnol. Oceanogr. 18, 897–907.
Meinshausen, M., Smith, S.J., Calvin, K., Daniel, J.S., Kainuma, M.L.T., Lamarque, J.-F., Matsumoto, K., Montzka, S.A., Raper, S.C.B., Riahi, K., Thomson, A., Velders, G.J.M., van Vurren, D.P.P., 2011. The RCP greenhouse gas concentrations and their extensions from 1765 to 2300. Clim. Chang. 109, 213–241.
Mercurio, P., Mueller, J.F., Eaglesham, G., Flores, F., Negri, A.P., 2015. Herbicide persistence in seawater simulation experiments. PLoS One 10, e0136391.
Mercurio, P., Mueller, J.F., Eaglesham, G., O'Brien, J., Flores, F., Negri, A.P., 2016. Degradation of herbicides in the tropical marine environment: influence of light and sediment. PLoS One 11, 11.
Moretto, J.A.S., Furlan, J.P.R., Fernandes, A.F., Bauermeister, A., Lopes, N.P., Stehling, E. G., 2019. Alternative biodegradation pathway of the herbicide diuron. Int. Biodeterior. Biodegradation 143, 104716.
Negri, A.P., Vollhardt, C., Humphrey, C., Heyward, A., Jones, R., Eaglesham, G., Fabricius, K., 2005. Effects of the herbicide diuron on the early life history stages of coral. Mar. Pollut. Bull. 51, 370–383.
Negri, A.P., Flores, F., Röthig, T., Uthicke, S., 2011. Herbicides increase the vulnerability of corals to rising sea surface temperature. Limnol. Oceanogr. 56, 471–485.
Negri, A.P., Flores, F., Mercurio, P., Mueller, J.F., Collier, C.J., 2015. Lethal and sub-lethal chronic effects of the herbicide diuron on seagrass. Aquat. Toxicol. 165, 73–83.
Negri, A.P., Smith, R.A., King, O., Frangos, J., Warne, M.St.J., Uthicke, S., 2020. Adjusting tropical marine water quality guideline values for elevated ocean temperatures. Environ. Sci. Technol. 54, 1102–1110.
Noonan, S.H.C., Fabricius, K.E., 2016. Ocean acidification affects productivity but not the severity of thermal bleaching in some tropical corals. ICES J. Mar. Sci. 73, 715–726.
O'Brien, D., Lewis, S., Davis, A., Gallen, C., Smith, R., Turner, R., Warne, M.St.J., Turner, S., Caswell, S., Mueller, J.F., Brodie, J., 2016. Spatial and temporal variability in pesticide exposure downstream of a heavily irrigated cropping area: application of different monitoring techniques. J. Agric. Food Chem. 64, 3975–3989.
Oettmeier, W., 1992. Herbicides of photosystem II. In: Barber, J. (Ed.), The Photosystems: Structure, Function and Molecular Biology. Elsevier, Amsterdam, pp. 349–408.
Pierrot, D., Lewis, E., Wallace, D.W.R., 2006. MS Excel Program Developed for CO2 System Calculations. ORNL/CDIAC-105a. Carbon Dioxide Information Analysis Center, Oak Ridge National Laboratory, U.S. Department of Energy, Oak Ridge, Tennessee.
Pulver, E.L., Ries, S.K., 1973. Action of simazine in increasing plant protein content. Weed Sci. 21, 233–237.
R Core Team, 2020. R: A Language and Environment for Statistical Computing. R Foundation for Statistical Computing, Vienna, Austria. URL https://www.R-project.org/.
Ralph, P.J., Smith, R.A., Macinnis-Ng, C.M.O., Seery, C.R., 2007. Use of fluorescence-based ecotoxicological bioassays in monitoring toxicants and pollution in aquatic systems: review. Toxicol. Environ. Chem. 89, 589–607.
Ries, S.K., Chmiel, H., Dilley, D.R., Filner, P., 1967. Increase in nitrate reductase activity and protein content of plants treated with simazine. Proc. Natl. Acad. Sci. 58, 526–532.
Roubeix, V., Mazzella, N., Schouler, L., Fauvelle, V., Morin, S., Coste, M., Delmas, F., Margoum, C., 2011. Variations of periphytic diatom sensitivity to the herbicide diuron and relation to species distribution in a contamination gradient: implications for biomonitoring. J. Environ. Monit. 13, 1768–1774.
Rueden, C.T., Schindelin, J., Hiner, M.C., 2017. ImageJ2: ImageJ for the next generation of scientific imaging data. BMC Bioinform. 18.
Schindelin, J., Rueden, C.T., Hiner, M.C., 2015. The ImageJ ecosystem: an open platform for biomedical image analysis. Mol. Reprod. Dev. PMID 26153368.
Schneider, K., Erez, J., 2006. The effect of carbonate chemistry on calcification and photosynthesis in the hermatypic coral *Acropora eurystoma*. Limnol. Oceanogr. 51, 1284–1293.
Siebeck, U., Marshall, N., Klüter, A., Hoegh-Guldberg, O., 2006. Monitoring coral bleaching using a colour reference card. Coral Reefs 25, 453–460.
Smith, R., Middlebrook, R., Turner, R., Huggins, R., Vardy, S., Warne, M.St.J., 2012. Large-scale pesticide monitoring across Great Barrier Reef catchments – Paddock to Reef Integrated Monitoring, Modelling and Reporting Program. Mar. Pollut. Bull. 65, 117–127.
Smithson, M., Verkuilen, J., 2006. A better lemon squeezer? Maximum-likelihood regression with beta-distributed dependent variables. Psychol. Methods 11, 54–71.
Stimson, J., Kinzie, R.A., 1991. The temporal pattern and rate of release of zooxanthellae from the reef coral *Pocillopora damicornis* (Linnaeus) under nitrogen-enrichment and control conditions. J. Exp. Mar. Biol. Ecol. 153, 63–67.
Strahl, J., Stolz, I., Uthicke, S., Vogel, N., Noonan, S.H.C., Fabricius, K.E., 2015. Physiological and ecological performance differs in four coral taxa at a volcanic carbon dioxide seep. Comp. Biochem. Physiol. A 179–186.
Thomas, M.C., Flores, F., Kaserzon, S., Fisher, R., Negri, A.P., 2020a. Toxicity of ten herbicides to the tropical marine microalgae *Rhodomonas salina*. Sci. Rep. 10, 7612.
Thomas, M.C., Flores, F., Kaserzon, S., Reeks, T.A., Negri, A.P., 2020b. Toxicity of the herbicides diuron, propazine, tebuthiuron, and haloxyfop to the diatom *Chaetoceros muelleri*. Sci. Rep. 10, 19592.
Uthicke, S., Fabricius, K.E., 2012. Productivity gains do not compensate for reduced calcification under near-future ocean acidification in the photosynthetic benthic foraminifer species *Marginopora vertebralis*. Glob. Chang. Biol. 18, 2781–2791.
van Dam, J.W., Negri, A.P., Mueller, J.F., Altenburger, R., Uthicke, S., 2012. Additive pressures of elevated sea surface temperatures and herbicides on symbiont-bearing foraminifera. PLoS One 7, e33900.
Vandermeulen, J.H., Davis, N.D., Muscatine, L., 1972. The effect of inhibitors of photosynthesis on zooxanthellae in corals and other marine invertebrates. Mar. Biol. 16, 185–191.
Vehtari, A., Gelman, A., Gabry, J., 2017. Practical Bayesian model evaluation using leave-one-out cross-validation and WAIC. Stat. Comput. 27, 1413–1432.
Vehtari, A., Gabry, J., Magnusson, M., Yao, Y., Bürkner, P., Paananen, T., Gelman, A., 2020. loo: efficient leave-one-out cross-validation and WAIC for Bayesian models. R package version 2.3.1. https://mc-stan.org/loo.
Warne, M.St.J., King, O., Smith, R.A., 2018. Ecotoxicity thresholds for ametryn, diuron, hexazinone and simazine in fresh and marine waters. Environ. Sci. Pollut. Res. 25, 3151–3169.
Warne, M.St.J., Smith, R.A., Turner, R.D.R., 2020. Analysis of pesticide mixtures discharged to the lagoon of the Great Barrier Reef, Australia. Environ. Pollut. 265, 114088.
Wilkinson, A.D., Collier, C.J., Flores, F., Negri, A.P., 2015. Acute and additive toxicity of ten photosystem-II herbicides to seagrass. Sci. Rep. 5, 17443.
Wilkinson, A.D., Collier, C.J., Flores, F., Langlois, L., Ralph, P.J., Negri, A.P., 2017. Combined effects of temperature and the herbicide diuron on photosystem II activity of the tropical seagrass *Halophila ovalis*. Sci. Rep. 7, 45404.
Wuebbles, D.J., Fahey, D.W., Hibbard, K.A., Arnold, J.R., DeAngelo, B., Doherty, S., Esterling, D.R., Edmonds, J., Edmonds, T., Hall, T., Hayhoe, K., Huffman, F.M., Horton, R., Huntzinger, D., Jewett, L., Knutson, T., Kopp, R.E., Kossin, J.P., Kunkel, K.E., LeGrande, A.N., Leung, L.R., Maslowski, W., Mears, C., Perlwitz, J., Romanou, A., Sanderson, B.M., Sweet, W.V., Taoylor, P.C., Trapp, R.J., Vose, R.S., Waliser, D. E., Wehner, M.F., West, T.O., Alley, R., Armstrong, C.T., Bruno, J., Busch, S., Champion, S., Durre, I., Gledhill, D., Goldstein, J., Huang, B., Krishnan, H., Levin, L., Muller-Karger, F., Rhoades, A., Stevens, L., Sun, L., Takle, E., Ullrich, P., Wahl, E., Walsh, J., 2017. Climate Science Special Report: Fourth National Climate Assessment (NCA4), Volume I. Agronomy Reports 8, https://lib.dr.iastate.edu/agron_reports/8.